Structural and Chemical Characterization of Layered $Li_{1-x}Ni_{1-y}Mn_yO_{2-\delta}$ ($y = 0.25$ and 0.5, and $0 \leq (1 - x) \leq 1$) Oxides

S. Venkatraman and A. Manthiram*

Materials Science and Engineering Program, 1 University Station C2200, The University of Texas at Austin, Austin, Texas 78712

Received August 15, 2003. Revised Manuscript Received October 24, 2003

Lithium has been chemically extracted from the O3-type layered $LiNi_{1-y}Mn_yO_2$ ($y = 0.25$ and 0.5) oxides with the oxidizer NO_2BF_4 in acetonitrile medium, and the products $Li_{1-x}Ni_{1-y}Mn_yO_2$ ($0 \leq (1 - x) \leq 1$) have been characterized by X-ray diffraction, redox titrations, and infrared spectroscopy. Rietveld refinement of the X-ray diffraction data indicates that the $Li_{1-x}Ni_{0.5}Mn_{0.5}O_{2-\delta}$ system maintains the parent O3-type structure without the formation of any new phases for the entire lithium content $0 \leq (1 - x) \leq 1$. In contrast, the $Li_{1-x}Ni_{0.75}Mn_{0.25}O_{2-\delta}$ system begins to form a new O3′ phase with a smaller *c* parameter for $(1 - x) < 0.29$, a two-phase region consisting of O3 and O3′ phases for $0 < (1 - x) < 0.29$, and a single phase O3′ phase for $x = 0$. Wet-chemical redox titration analysis indicates that the $y = 0.5$ system has a greater tendency to lose oxygen from the lattice than the $x = 0.25$ sample due to a greater overlap of the metal:3d band with top of the O^{2-}:2p band, which is consistent with the observed voltage profiles. Nevertheless, both the systems remain as semiconductors for the entire $0 \leq (1 - x) \leq 1$. The results are compared with those found before for the $Li_{1-x}CoO_{2-\delta}$ and $Li_{1-x}Ni_{0.85}Co_{0.15}O_{2-\delta}$ systems.

Introduction

Commercial lithium-ion batteries currently use $LiCoO_2$ as the cathode, which adopts the O3-type layered structure shown in Figure 1. However, only 50% of the theoretical capacity of $LiCoO_2$ could be practically used, and Co is expensive and relatively toxic. These drawbacks have created interest in the development of alternate cathode materials. In this regard, layered $LiNiO_2$ and $LiMnO_2$ are appealing as Ni and Mn are less expensive and less toxic than Co. However, $LiNiO_2$ suffers from the difficulty of synthesizing it as a perfectly ordered phase,[1,2] Jahn−Teller distortion associated with the single electron in the e_g orbitals of the low-spin Ni^{3+}:$3d^7$ ion,[3,4] irreversible phase transitions occurring during the charge−discharge process,[5,6] and the migration of Ni^{3+} ions from the nickel plane to the lithium plane at elevated temperatures.[7,8] Some of these difficulties could be suppressed by a partial substitution of Co for Ni, and compositions such as $LiNi_{0.85}Co_{0.15}O_2$ show improved electrochemical performance.[9−11] Unfortunately, the nickel-rich $LiNi_{1-y}Co_yO_2$ system suffers from the development of impedance at elevated temperatures, possibly due to the cation migrations.[12]

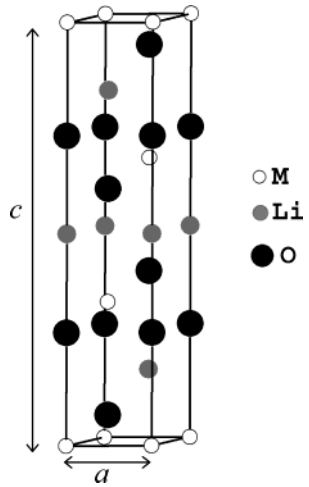

Figure 1. Crystal structure of the ideal O3-type $LiMO_2$ having an oxygen stacking sequence of ....ABCABC.... along *c*-axis.

$LiMnO_2$ made by conventional high-temperature procedures, on the other hand, does not adopt the O3-type structure shown in Figure 1. Instead, it adopts a

* To whom correspondence should be addressed. Phone 512-471-1791. Fax: 512-471-7681. E-mail: rmanth@mail.utexas.edu.

(1) Dutta, G.; Manthiram, A.; Goodenough, J. B. *J. Solid State Chem.* **1992**, *96*, 123.
(2) Kanno, R.; Kubo, H.; Kawamoto, Y.; Kamiyama, T.; Izumi, F.; Takeda, Y.; Takano, M. *J. Solid State Chem.* **1994**, *110*, 216.
(3) Nakai, I.; Nakagome, T. *Electrochem. Solid State Lett.* **1998**, *1*, 259.
(4) Nakai, I.; Takahashi, K.; Shiraishi, Y.; Nakagome, T.; Nishikawa, F. *J. Solid State Chem.* **1998**, *140*, 145.
(5) Ohzuku, T.; Ueda, A.; Nagayama, M.; Iwakashi, Y.; Komori, H. *Electrochim. Acta* **1993**, *38*, 1159.
(6) Amatucci, G. G.; Tarascon, J. M.; Klein, L. C. *J. Electrochem. Soc.* **1996**, *143*, 1114.
(7) Chebiam, R. V.; Prado, F.; Manthiram, A. *J. Electrochem. Soc.* **2001**, *148*, A49.
(8) Choi, S.; Manthiram, A. *J. Electrochem. Soc.* **2002**, *149*, A1157.
(9) Delmas, C.; Saadoune, I.; Rougier, A. *J. Power Sources* **1995**, *43−44*, 595.
(10) Ueda, A.; Ohzuku, T. *J. Electrochem. Soc.* **1994**, *141*, 2010.
(11) Li, W.; Currie J. C. *J. Electrochem. Soc.* **1997**, *144*, 2773.
(12) Nagasubramanian, G. *Proceedings of the 40th Power Sources Conference*, Cherry Hill, NJ, June 10−13, 2002; p 434.

10.1021/cm034757b CCC: $25.00
Published on Web 11/22/2003

thermodynamically more stable orthorhombic structure. However, the O3-type $LiMnO_2$ could be obtained by an ion exchange reaction of $NaMnO_2$ with lithium salts.[13] Unfortunately, the layered $LiMnO_2$ is plagued by a migration of the manganese ions from the manganese plane to the lithium plane and the consequent formation of spinel-like phases during the electrochemical charge−discharge process.[14,15]

Interestingly, the composition $LiNi_{0.5}Mn_{0.5}O_2$ has recently been shown to not form spinel-like phases during cycling.[16] In fact, $Li_{0.5}Ni_{0.5}Mn_{0.5}O_2$ does not transform to spinel-like phase even after heating at 200 °C, whereas both the end members $Li_{0.5}MnO_2$ and $Li_{0.5}NiO_2$ transform to spinel-like phases at room temperature and 150 °C, respectively.[8] The remarkable structural stability of $Li_{1-x}Ni_{0.5}Mn_{0.5}O_2$ has been attributed to (i) the absence of Mn^{3+} as $LiNi_{0.5}Mn_{0.5}O_2$ has been shown to consist of Mn^{4+} and Ni^{2+} ions[17] and (ii) the presence of mixed cations in the transition metal planes and the consequent perturbation of the cooperativity among the transition metal ions.[8] With a good structural stability, the $LiNi_{0.5}Mn_{0.5}O_2$ system has been shown to exhibit a reversible capacity of 150−200 mAh/g depending on the synthesis conditions,[18−20] which is higher than that found for $LiCoO_2$ (140 mAh/g) but close to that of $LiNi_{0.85}Co_{0.15}O_2$ (180 mAh/g).

Our group has been recently focusing on understanding the factors that limit the practical capacities of layered oxides crystallizing in the O3-type structure (Figure 1), and we attributed the difference in capacity between the $LiCoO_2$ and $LiNi_{0.85}Co_{0.15}O_2$ systems to the differences in their chemical stability and the lithium content at which the lattice tends to lose oxygen.[21−23] The chemical instability was ascertained by monitoring the variations of the oxygen contents of the chemically delithiated samples with lithium content. The lithium content at which oxygen loss begins to occur was also found to be accompanied by the formation of a new phase and/or a decrease in the *c* lattice parameter. We present here an extension of similar studies to the system $LiNi_{1-y}Mn_yO_2$ ($y = 0.25$ and 0.5) with an aim to understand the differences in practical capacities among the three systems: $LiCoO_2$, $LiNi_{0.85}Co_{0.15}O_2$, and $LiNi_{0.5}Mn_{0.5}O_2$. The products obtained by chemically extracting lithium from $LiNi_{1-y}Mn_yO_2$ are characterized by X-ray diffraction, oxygen content analysis with a redox titration, and electrical conduction analysis with infrared spectroscopy.

Experimental Section

The $LiNi_{1-y}Mn_yO_2$ ($y = 0.25$ and 0.5) samples were synthesized by a coprecipitation procedure. Stoichiomeric amounts of nickel(II) acetate (99+%, Alfa Aesar) and manganese(II) acetate (99+%, Acros Organics) were dissolved in deionized water and added drop by drop into a 0.1 M KOH (laboratory grade, Fischer Scientific) solution to coprecipitate the metal ions as hydroxides. The coprecipitate was then filtered, washed with deionized water, and dried overnight at 100 °C in an air oven. The coprecipitate of nickel and manganese was then ground with a required amount of $LiOH·H_2O$ (laboratory grade, Fischer Scientific) and fired first at 480 °C for 3 h and then at 900 °C for 3 h in air for $y = 0.5$[18] and at 850 °C for 24 h in oxygen for $y = 0.25$.

Chemical extraction of lithium was carried out by stirring the $LiNi_{1-y}Mn_yO_2$ powders in an acetonitrile solution of NO_2BF_4 for 2 days under argon atm using a Schlenk line:

$$LiNi_{1-y}Mn_yO_2 + xNO_2BF_4 \rightarrow Li_{1-x}Ni_{1-y}Mn_yO_2 + xNO_2 + xLiBF_4 \quad (1)$$

$Li_{1-x}Ni_{1-y}Mn_yO_2$ compositions with various values of lithium contents ($1 - x$) could be obtained by controlling the molar ratio of $LiNi_{1-y}Mn_yO_2$:NO_2BF_4 in the initial reaction mixture. Because of the high reactivity of NO_2BF_4 and the possibilities of its decomposition prior to use and side reactions, the experiments invariably required excess amounts of the oxidizer than would be expected based on reaction 1 to achieve a specific value of lithium content ($1 - x$) in $Li_{1-x}Ni_{1-y}Mn_yO_2$. The products formed after the reaction were washed 3 times with acetonitrile under argon to remove $LiBF_4$ and dried under vacuum at ambient temperature. After drying, the reaction flasks were opened in an argon-filled glovebox.

The lithium contents were determined by atomic absorption spectroscopy. The oxidation state of the transition metal ions and the oxygen contents were determined by iodometric titration,[24] which was carried out immediately after taking the samples out of the argon-filled glovebox. Structural characterizations were carried out with X-ray powder diffraction using Cu Kα radiation. The X-ray diffraction data were collected from $2\theta = 10$ to 80° with a counting time of 10 s per 0.02° using a Philips 3550 diffractometer. Structural refinements and lattice parameter determinations were carried out by analyzing the X-ray diffraction data with the Rietveld method using the DBWS-9411 PC program.[25] Fourier transform infrared (FTIR) spectra were recorded with pellets made with KBr and the sample. Electrochemical extraction of lithium was achieved by charging the CR2032 coin cells assembled with the $LiNi_{1-y}Mn_yO_2$ cathode, lithium anode, and 1 M $LiPF_6$ in ethylene carbonate (EC) and diethyl carbonate (DEC) electrolyte at C/100 rate. The cathodes were fabricated by mixing 75 wt % active material powder with 20 wt % acetylene black and 5 wt % of poly(tetrafluoroethylene) (PTFE) binder.

Results and Discussion

Crystal Chemistry. The X-ray diffraction data of the parent $LiNi_{1-y}Mn_yO_2$ ($y = 0.25$ and 0.5) samples were first fitted with a strict two-dimensional model based on the O3-type structure (Figure 1),[26] $[Li]_{3a}(Ni_{1-y}Mn_y)_{3b}\{O_2\}_{6c}$, in which no cation mixing (Li^+ in $(Ni,Mn)^{n+}$ planes or $(Ni,Mn)^{n+}$ in Li^+ planes) was allowed. Such a fitting resulted in negative values for the atomic displacement parameter B_{Li}, indicating the existence of

(13) Armstrong, A. R.; Bruce P. G. *Nature* **1996**, *381*, 499.
(14) Wang, H.; Jang, Y.-I.; Chiang, Y.-M. *Mater. Res. Soc. Symp. Proc.* **1999**, *548*, 143.
(15) Shao-Horn, Y.; Hackney, S. A.; Armstrong, A. R.; Bruce, P. G.; Gitzendanner, R.; Johnson, C. S.; Thackeray, M. M. *J. Electrochem. Soc.* **1999**, *146*, 2404.
(16) Ohzuku, T.; Makimura, Y. *Chem. Lett.* **2001**, 744.
(17) Reed, J.; Ceder, G. *Electrochem. Solid State Lett.* **2002**, *5*, A145.
(18) Lu, Z.; Macneil, D. D.; Dahn, J. R. *Electrochem. Solid State Lett.* **2001**, *4*, A191.
(19) Yang, X.-Q.; McBreen, J.; Yoon, W.-S.; Grey, C. P. *Electrochem. Commun.* **2002**, *4*, 649.
(20) Yoon, W.-S.; Paik, Y.; Yang, X.-Q.; Balasubramanian, M.; McBreen, J.; Grey, C. P. *Electrochem. Solid State Lett.* **2002**, *5*, A163.
(21) Chebiam, R. V.; Prado, F.; Manthiram, A. *Chem. Mater.* **2001**, *13*, 2951.
(22) Venkatraman, S.; Manthiram, A. *Chem. Mater.* **2002**, *14*, 3907.
(23) Venkatraman, S.; Shin, Y.; Manthiram, A. *Electrochem. Solid State Lett.* **2003**, *6*, A9.
(24) Manthiram, A.; Swinnea, S.; Siu, Z.; Steinfink, H.; Goodenough, J. B. *J. Am. Chem. Soc.* **1987**, *109*, 6667.
(25) Young, R. A.; Shakthivel, A.; Moss, T. S.; Paiva Santos, C. O. *J. Appl. Crystallogr.* **1995**, *28*, 366.
(26) Akimoto, J.; Gotoh, Y.; Oosawa, Y. *J. Solid State Chem.* **1998**, *141*, 298.

Table 1. Structural Parameters of $LiNi_{0.75}Mn_{0.25}O_2$[a]

atom	site	*x*	*y*	*z*	occupancy
Li (1)	3a	0	0	0	0.918
Ni (1)	3a	0	0	0	0.082
Mn (1)	3b	0	0	0.5	0.250
Ni (2)	3b	0	0	0.5	0.668
Li (2)	3b	0	0	0.5	0.082
O (1)	6c	0	0	0.2425(3)	2.000

[a] Space group: $R\bar{3}m$ (S.G. 166); $a = 2.8844(0)$ Å, $c = 14.2438(4)$ Å, $V = 102.629(4)$ Å^3. R_{wp}= 9.12%, R_p = 6.94, S = 3.34. Constraints: $n(\mathrm{Li})_{3a} + n(\mathrm{Ni})_{3a} = 1$; $n(\mathrm{Li})_{3b} + n(\mathrm{Ni})_{3b} + n(\mathrm{Mn})_{3b} = 1$.

Table 2. Structural Parameters of $LiNi_{0.5}Mn_{0.5}O_2$[a]

atom	site	*x*	*y*	*z*	occupancy
Li (1)	3a	0	0	0	0.882
Ni (1)	3a	0	0	0	0.118
Mn (1)	3b	0	0	0.5	0.500
Ni (2)	3b	0	0	0.5	0.381
Li (2)	3b	0	0	0.5	0.118
O (1)	6c	0	0	0.2441(3)	2.000

[a] Space group: $R\bar{3}m$ (S.G. 166); $a = 2.8879(1)$ Å, $c = 14.269(1)$ Å, $V = 103.066(9)$ Å^3. R_{wp}= 8.85%, R_p = 6.94, S = 2.30. Constraints: $n(\mathrm{Li})_{3a} + n(\mathrm{Ni})_{3a} = 1$; $n(\mathrm{Li})_{3b} + n(\mathrm{Ni})_{3b} + n(\mathrm{Mn})_{3b} = 1$.

excess electron density in the lithium plane and cation mixing.[27] The refinement was then carried out with a model, in which a fraction of the Ni^{2+} ions was allowed to be in the lithium plane, $[Li_{1-z}Ni_z]_{3a}(Ni_{1-y-z}Mn_y\,Li_z)_{3b}\{O_2\}_{6c}$. In this model, only Ni^{2+} and no Mn^{4+} was allowed to be in the lithium plane because neutron diffraction studies[28,29] on similar compositions have indicated the presence of only $Ni^{2+}$and not Mn^{4+} in the lithium layer. This model led to a nickel content z = 0.082 for y = 0.25 and z = 0.112 for y = 0.5 in the lithium plane as seen in Tables 1 and 2. Figure 2 shows the Rietveld fitting based on this model, in which the observed and calculated X-ray diffraction patterns and the difference between them are shown for both the $LiNi_{1-y}Mn_yO_2$ (y = 0.25 and 0.5) samples. The data thus reveal considerable cation mixing in the initial $LiNi_{1-y}Mn_yO_2$ samples, which is consistent with the previous literature reports.[28,29]

Figure 3 shows the evolution of the X-ray diffraction patterns of the $Li_{1-x}Ni_{0.75}Mn_{0.25}O_2$ system for $0 \le (1 - x) \le 1$. While the system remains as a single phase material with the initial O3-type structure for $(1 - x) \ge 0.29$, a new phase begins to appear for $(1 - x) < 0.29$ as indicated by the presence of a shoulder on the right side of the (003) reflection in the $(1 - x) = 0.25$ sample, which becomes clear in the enlarged (003) reflection shown on the right side of Figure 3. The intensity of the reflection corresponding to the new phase grows with further decrease in lithium content, and the end member $Ni_{0.75}Mn_{0.25}O_2$ consists of only the new phase. However, the new phase could also be indexed on the basis of the O3-type structure, but with a smaller c lattice parameter, and we designate this new phase as O3′ phase. Both the O3 and O3′ phases coexist in the region $0 < (1 - x) \le 0.25$. The crystal chemistry of the

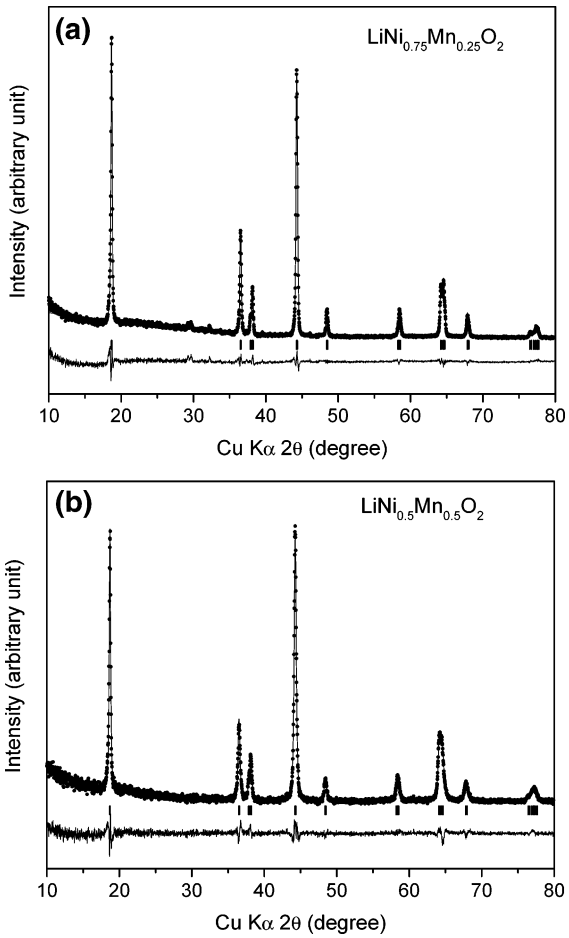

Figure 2. Observed (●) and calculated (−) X-ray diffraction data and the difference between them for $LiNi_{0.75}Mn_{0.25}O_2$ (a) and $LiNi_{0.5}Mn_{0.5}O_2$ (b). The positions of the reflections are also indicated.

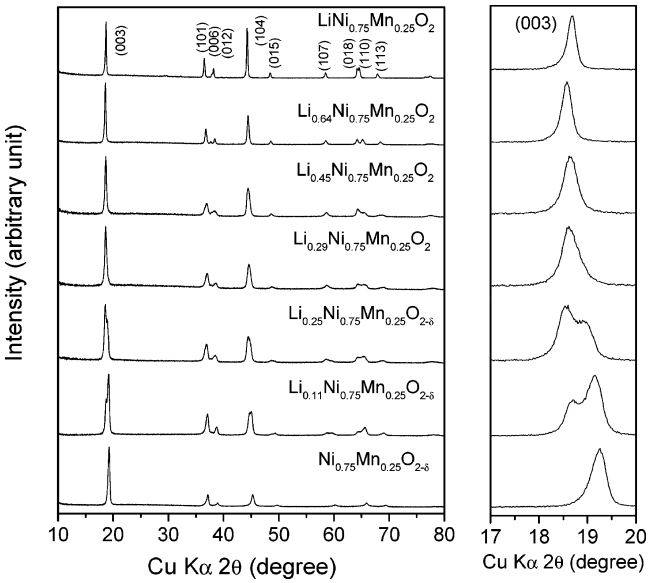

Figure 3. Evolution of the X-ray diffraction patterns of $Li_{1-x}Ni_{0.75}Mn_{0.25}O_{2-\delta}$ for $0 \le (1 - x) \le 1$.

chemically delithiated $Li_{1-x}Ni_{0.75}Mn_{0.25}O_2$ samples is similar to that of the $Li_{1-x}Ni_{0.85}Co_{0.15}O_2$ system, in which the O3 and O3′ phases coexist for $0 < (1 - x) \le 0.25$.[23]

Figure 4 shows the evolution of the X-ray diffraction patterns of the $Li_{1-x}Ni_{0.5}Mn_{0.5}O_2$ system for $0 \le (1 - x) \le 1$. This system maintains the initial O3-type structure

(27) Rougier, A.; Gravereau, P.; Delmas, C. *J. Electrochem. Soc.* **1996**, *143*, 1168.
(28) Lu, Z.; Beaulieu, L. Y.; Donaberger, R. A.; Thomas, C. L.; Dahn, J. R. *J. Electrochem. Soc.* **2002**, *149*, A778.
(29) Kobayashi, H.; Sakaebe, H.; Kageyama, H.; Tatsumi, K.; Arachi, Y.; Kamiyama, T. *J. Mater. Chem.* **2003**, *13*, 590.

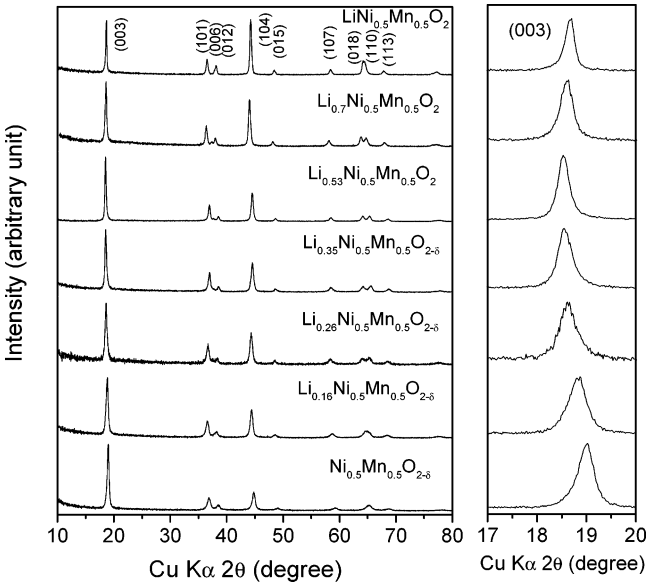

Figure 4. Evolution of the X-ray diffraction patterns of $Li_{1-x}Ni_{0.5}Mn_{0.5}O_{2-\delta}$ for $0 \leq (1 - x) \leq 1$.

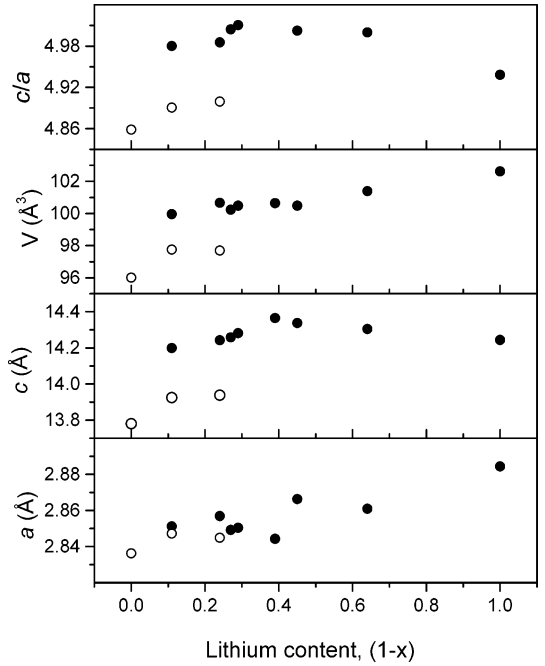

Figure 5. Variations of the unit cell parameters of $Li_{1-x}Ni_{0.75}Mn_{0.25}O_{2-\delta}$ with lithium content $(1 - x)$. The closed (●) and open (○) symbols refer, respectively, to the O3 and O3′ phases.

without the formation of any new phase and remains as a single phase material for the entire $0 \leq (1 - x) \leq 1$ in contrast to the $y = 0.25$ system. The enlarged pattern shown on the right side of Figure 4 clearly rules out the formation of any new phase. The observation of single phase for the entire lithium content $0 \leq (1 - x) \leq 1$ is consistent with that reported for $Li_{0.2}Ni_{0.5}Mn_{0.5}O_2$,[30] but in contrast to the additional H2 phase reported by Yang et al.[19] However, while the samples in this study are prepared by chemical delithiation, the previous literature data refer to samples prepared by electrochemical delithiation. Any difference seen between the chemically and electrochemically delithiated samples could be due to the differences in the charging rate. Whereas electrochemical charging is generally carried out at a slow rate (< C/2), the chemical delithiation can occur rapidly with rates as high as >4C as we have noticed before with the $LiCoO_2$ system.[22] In the chemical delithiation experiments, the entire amount of the oxidizer is added in a single step, and therefore, delithiation would take place at the maximum possible rate and could lead to kinetically more stable phases. In contrast, the slow electrochemical charging rates can lead to thermodynamically more stable phases. We are currently working on the kinetics of chemical delithiation using NO_2BF_4, and the preliminary results indicate that the rate of delithiation depends on the degree of cation disorder in the layered $LiMO_2$ oxides.

Comparing the crystal chemistry of the various chemically delithiated layered oxide systems we have investigated so far, $Li_{1-x}Ni_{0.5}Mn_{0.5}O_2$ is the only system that remains as a single O3-phase material for the entire lithium content $0 \leq (1 - x) \leq 1$. While both $Li_{1-x}Ni_{0.85}Co_{0.15}O_2$ and $Li_{1-x}Ni_{0.75}Mn_{0.25}O_2$ form the new O3′ phase for $(1 - x) \leq 0.25$,[23] $Li_{1-x}CoO_2$ forms initially the new metastable P3 phase for $(1 - x) \leq 0.45$ by a gliding of the CoO_2 sheets, which on prolonged reaction time with the oxidizer slowly transforms to the O1 phase with further gliding of the CoO_2 sheets.[22] It is possible that the presence of a significant amount of an electrochemically inactive ion such as Mn^{4+} may play a role in controlling the crystal chemistry of the delithiated (charged) layered oxide compositions. A systematic future investigation of the crystal chemistry of the various chemically delithiated cation-substituted layered oxide compositions can enhance our understanding of this issue. Another important point to note is that the $[LiO_6]$ octahedra, if any, will share not only edges, but also faces with the $[CoO_6]$ octahedra in the P3 and O1 structures, and the electrostatic repulsion between any $M^{3+/4+}$ ions present in the lithium planes and the $M^{3+/4+}$ ions in the transition metal planes across the shared faces can destabilize the P3 and O1 structures. It is possible that the absence of cation mixing in $LiCoO_2$ may allow the formation of P3 and O1 phases, while the presence of some cation mixing in $Li_{1-x}Ni_{0.85}Co_{0.15}O_2$ and $Li_{1-x}Ni_{0.75}Mn_{0.25}O_2$ may prevent their formation.

Figure 5 shows the variations of the unit cell parameters with lithium content $(1 - x)$ for $Li_{1-x}Ni_{0.75}Mn_{0.25}O_2$. The *c* parameter increases due to an increasing electrostatic repulsion between the oxide ion across the van der Waals gap and the *a* parameter decreases with decreasing lithium content in the region $0.29 \leq (1 - x) \leq 1$ where the initial O3-type structure is maintained. The formation of the new O3′ phase for $(1 - x) < 0.29$ is accompanied by a decrease in the *c* parameter. The variation of the *c*/*a* ratio follows the same trend as the *c* lattice parameter, and the unit cell volume decreases with decreasing lithium content.

Figure 6 shows the variations of the *a* and *c* lattice parameters with lithium content $(1 - x)$ for $Li_{1-x}Ni_{0.5}Mn_{0.5}O_2$. The *c* parameter increases and the *a* parameter decreases initially with decreasing lithium content in the region $0.4 \leq (1 - x) \leq 1$ similar to that found for the $y = 0.25$ sample in Figure 5. However, the trend reverses for $(1 - x) < 0.4$ although the initial O3

(30) Johnson, C. S.; Kim, J.-S.; Kropf, A. J.; Kahaian, A. J.; Vaughey, A. E.; Fransson, L. M. L.; Edstrom, K.; Thackeray, M. M. *Chem. Mater.* **2003**, *15*, 2313.

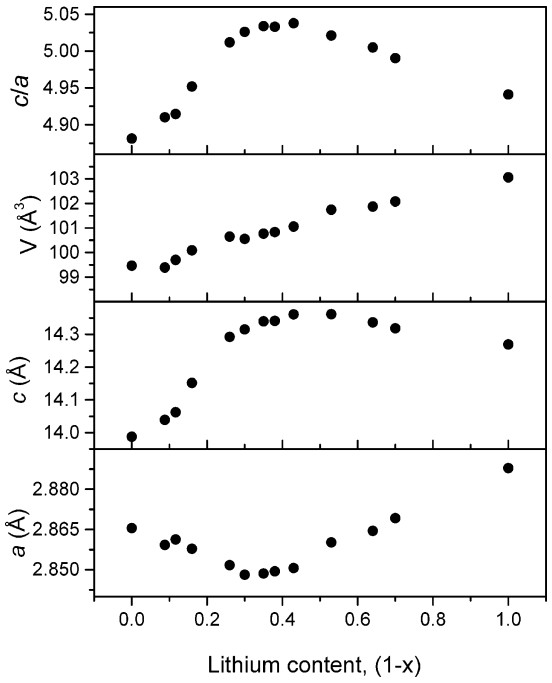

Figure 6. Variations of the unit cell parameters of $Li_{1-x}Ni_{0.5}Mn_{0.5}O_{2-\delta}$ with lithium content $(1 - x)$.

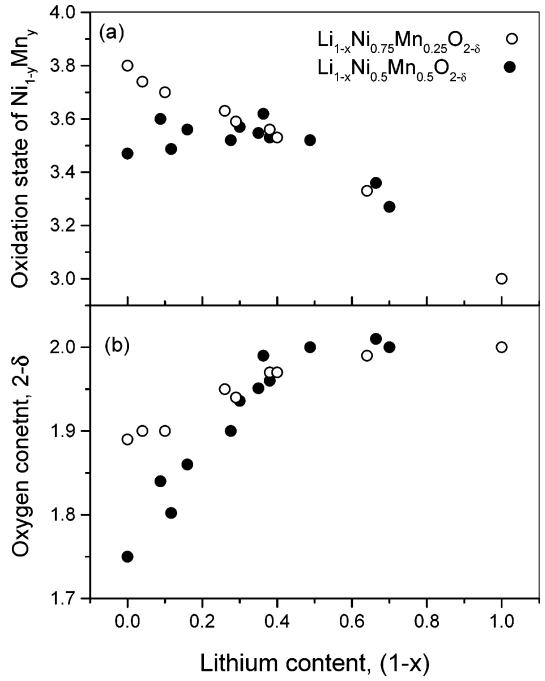

Figure 7. Variations of the (a) average oxidation state of $(Ni_{1-y}Mn_y)$ and (b) oxygen content with lithium content $(1 - x)$ for $Li_{1-x}Ni_{1-y}Mn_yO_{2-\delta}$ ($y = 0.25$ and 0.5).

structure is maintained without the formation of new phases for the entire $0 \le (1 - x) \le 1$. The variation of the *c*/*a* ratio follows the same trend as the *c* parameter and the unit cell volume decreases with decreasing lithium content similar to that found for the $y = 0.25$ sample in Figure 5.

The decrease in the *c* parameter observed at low lithium contents in $Li_{1-x}Ni_{1-y}Mn_yO_2$ is similar to that observed for many electrochemically charged layered $Li_{1-x}MO_2$ compositions.[6,31,32] The decrease in *c* parameter could be due to an increased O−O interaction across the van der Waals gap at low lithium contents, which

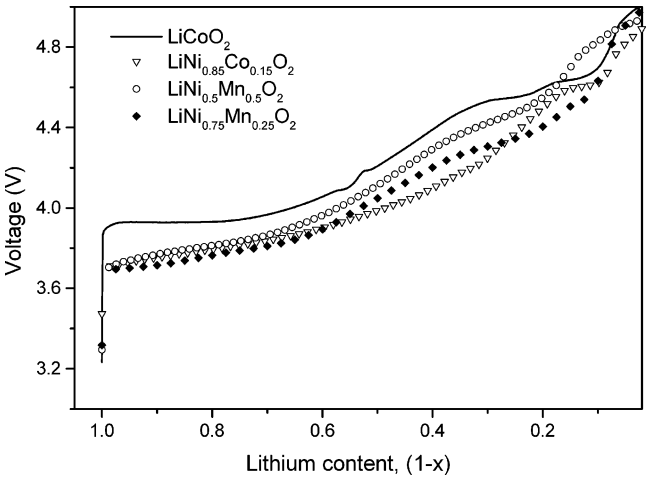

Figure 8. Comparison of the first charge profiles of the $LiCoO_2$, $LiNi_{0.85}C_{0.15}O_2$, $LiNi_{0.75}Mn_{0.25}O_2$, and $LiNi_{0.5}Mn_{0.5}O_2$ cathodes. The data were collected at C/100 rate.

in turn could be due to the introduction of holes into the O^{2-}:2p band[33] or the formation of oxygen vacancies[22,23] (see below).

Oxygen Content Analysis. Figure 7 shows the variations of the average oxidation state of the transition metal ions and the oxygen content with lithium content $(1 - x)$ for the chemically delithiated $Li_{1-x}Ni_{0.75}Mn_{0.25}O_{2-\delta}$ and $Li_{1-x}Ni_{0.5}Mn_{0.5}O_{2-\delta}$ for $0 \le (1 - x) \le 1$. The average oxidation state of $(Ni_{1-y}Mn_y)$ increases linearly with $(1 - x)$ and the oxygen content remains close to 2 for $0.3 \le (1 - x) \le 1.0$ in $Li_{1-x}Ni_{0.75}Mn_{0.25}O_{2-\delta}$. For $(1 - x) < 0.3$, the system tends to lose oxygen from the lattice, indicating chemical instability, and the end member $Ni_{0.75}Mn_{0.25}O_{2-\delta}$ has an oxygen content of 1.89. In contrast, the $Li_{1-x}Ni_{0.5}Mn_{0.5}O_{2-\delta}$ system tends to lose oxygen slightly earlier with the average oxidation state of $(Ni_{1-y}Mn_y)$ remaining nearly constant for $(1 - x) < 0.4$, and the end member $Li_{1-x}Ni_{0.5}Mn_{0.5}O_{2-\delta}$ has an oxygen content of 1.75. The loss of oxygen from the lattice implies an introduction of holes into the O^{2-}:2p band and a consequent oxidation of the oxide ions to oxygen at deep lithium extraction. Interestingly, the lithium content at which oxygen loss begins to occur coincides with the lithium content at which the *c* parameter begins to decrease as in the case of the $y = 0.5$ sample, or new phases (O3′ phase) with lower *c* parameter begin to form as in the case of the $y = 0.25$ sample. This observation is similar to that found before for both the $Li_{1-x}CoO_{2-\delta}$ and $Li_{1-x}Ni_{0.85}Co_{0.15}O_{2-\delta}$ systems,[23] and it reinforces the idea that the decrease in *c* parameter could be due to the increased O−O interaction caused by the introduction of holes into the O^{2-}:2p band.

Among the few $Li_{1-x}MO_{2-\delta}$ systems we have investigated so far, the M = Co,[23] $Ni_{0.85}Co_{0.15}$,[23] $Ni_{0.75}Mn_{0.25}$, and $Ni_{0.5}Mn_{0.5}$ systems begin to lose oxygen from the lattice, respectively, at $(1 - x) < 0.5$, 0.3, 0.4, and 0.3. The lithium content at which chemical instability sets in and the system begins to lose oxygen depends on the

(31) Ronci, F.; Scrosati, B.; Albertini, V. R.; Perfetti, P. *Electrochem. Solid State Lett.* **2000**, *3*, 174.
(32) Prado, G.; Fournès, L.; Delmas, C. *J. Solid State Chem.* **2001**, *159*, 103.
(33) Van der Ven, A.; Aydinol, M. K.; Ceder, G.; Kresse, G.; Hafner, J. *Phys. Rev. B* **1998**, *58*, 2975.

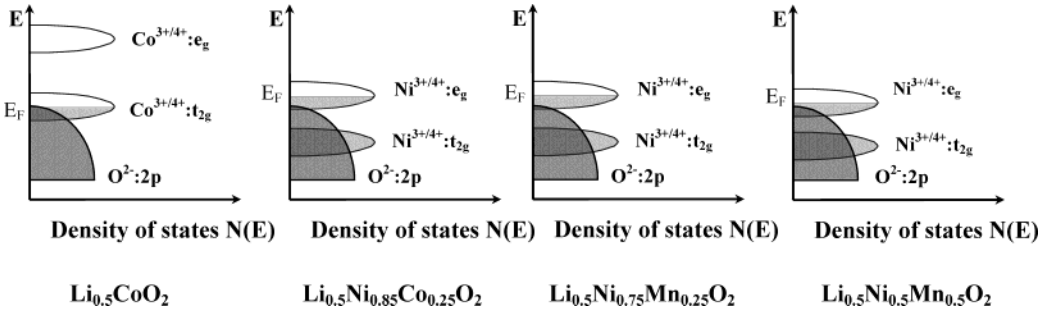

Figure 9. Qualitative energy diagrams for $Li_{0.5}CoO_2$, $Li_{0.5}Ni_{0.85}Co_{0.15}O_2$, $Li_{0.5}Ni_{0.75}Mn_{0.25}O_2$, and $Li_{0.5}Ni_{0.5}Mn_{0.5}O_2$.

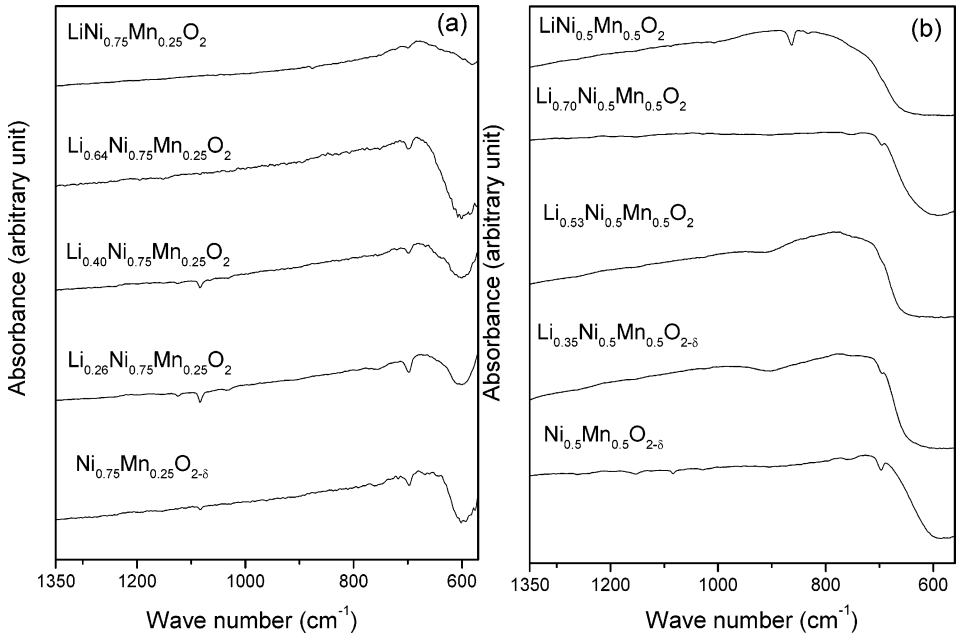

Figure 10. FTIR spectra of (a) $Li_{1-x}Ni_{0.75}Mn_{0.25}O_{2-\delta}$ and (b) $Li_{1-x}Ni_{0.5}Mn_{0.5}O_{2-\delta}$.

relative positions of the $M^{3+/4+}$:3d redox energy with respect to the top of the O^{2-}:2p band and the position of the Fermi energy E_F. Because the discharge−charge voltage profiles would be a reflection of the relative positions of E_F in different systems,[34] we decided to collect the first charge profiles of the various systems. Figure 8 compares the first charge profiles collected at a slow charging rate of C/100, which involves a charging time of 100 h to deintercalate all the lithium from $LiMO_2$. Such a very slow charging rate minimizes any possible polarization contributions to the voltage and ensures a profile close to that of open-circuit-voltage profiles. The observed voltage profiles in Figure 8 are consistent with the trend in the lithium content values at which oxygen loss begins to occur. The system with a higher charge voltage would be expected to experience greater chemical instability and lose oxygen earlier at a higher lithium content. Comparing the lithium contents at which oxygen loss begins to occur and the voltage profiles in Figure 8, one can conclude that the chemical instability in layered oxides sets in above ~4.25 V, which controls their practical capacity values. On the basis of this, one would expect reversible capacity values of around 140, 190, 180, and 160 mAh/g, respectively, for $LiCoO_2$, $LiNi_{0.85}Co_{0.15}O_2$, $LiNi_{0.75}Mn_{0.25}O_2$, and $LiNi_{0.5}Mn_{0.5}O_2$, which is consistent with the experimentally observed capacity values.

On the basis of the voltage profiles in Figure 8 and the lithium contents at which oxygen loss begins to occur, one can also propose a qualitative band diagram for the four $Li_{1-x}MO_2$ systems with M = Co, $Ni_{0.85}Co_{0.15}$, $Ni_{0.75}Mn_{0.25}$, and $Ni_{0.5}Mn_{0.5}$ (Figure 9). The system with a higher charge voltage at a given lithium content would have a greater lowering of the $M^{3+/4+}$:3d energy and a greater overlap between the $M^{3+/4+}$:3d and O^{2-}:2p bands, and consequently a greater tendency to lose oxygen from the lattice. As lithium is extracted from the system, when the Fermi energy E_F drops into the O^{2-}:2p band, the system will encounter chemical instability and tend to lose oxygen from the lattice. However, in the case of lithium-ion cells, the cathodes may not lose neutral oxygen, but instead may undergo reaction with the electrolyte.

Infrared Spectra. Figure 10 shows the Fourier transform infrared (FTIR) spectra of both the $Li_{1-x}Ni_{0.75}Mn_{0.25}O_{2-\delta}$ and $Li_{1-x}Ni_{0.5}Mn_{0.5}O_{2-\delta}$ samples. The FTIR spectra were recorded with the objective to get a qualitative idea of the conduction behavior (semiconducting or metallic) of these samples, as the chemically delithiated samples are metastable and are difficult to sinter to measure the electrical conductivity.[21,22] The spectra show characteristic absorption bands in the range 600−850 cm^{-1}, corresponding to the $(Ni_{1-y}Mn_y)$−O vibrations

(34) Delmas, C.; Menetrier, M.; Croguennec, L.; Levasseur, S.; Peres, J. P.; Pouillerie, C.; Prado, G.; Fournes, L.; Weill, F. *Int. J. Inorg. Mater.* **1999**, *1*, 11.

of the $(Ni_{1-y}Mn_y)O_6$ octahedra. The data reveal that both the systems $Li_{1-x}Ni_{0.75}Mn_{0.25}O_{2-\delta}$ and $Li_{1-x}Ni_{0.5}Mn_{0.5}O_{2-\delta}$ remain as semiconductors like the $Li_{1-x}Ni_{0.85}Co_{0.15}O_{2-\delta}$ system for the entire range of $0 \leq (1 - x) \leq 1$, unlike the $Li_{1-x}CoO_2$ system, which becomes metallic for $(1 - x) < 0.7$,[21,22,35] as indicated by the absence of absorption bands in $Li_{1-x}CoO_2$. In the case of metallic systems, the free electrons can oscillate to any incident wavelength, resulting in no characteristic absorption. Alternatively, a decreased optical skin depth of the incident beam in the case of metallic systems leads to a probing of only the surface of the sample and a consequent vanishing of the absorption bands. The semiconducting behavior of the $Li_{1-x}Ni_{1-y}Mn_yO_{2-\delta}$ systems is due to the completely filled t_{2g} bands, unlike the $Li_{1-x}CoO_2$ system that has a partially filled $Co^{3+/4+}$:t_{2g} band, providing a strong Co−Co interaction across the edge-shared CoO_6 octahedra.

Conclusions

Layered $Li_{1-x}Ni_{1-y}Mn_yO_{2-\delta}$ ($y = 0.25$ and 0.5) oxides have been synthesized for $0 \leq (1 - x) \leq 1$ by chemically extracting lithium from the corresponding $LiNi_{1-y}Mn_yO_2$ samples with NO_2BF_4 in acetonitrile medium. Although the $Li_{1-x}Ni_{0.5}Mn_{0.5}O_{2-\delta}$ system remains as a single-phase material with the initial O3-type structure for the entire lithium content $0 \leq (1 - x) \leq 1$, the $Li_{1-x}Ni_{0.75}Mn_{0.25}O_{2-\delta}$ system forms a new O3′ phase for $(1 - x) < 0.29$. The difference between the two systems could be due to the presence of a large amount of electrochemically inactive Mn^{4+} in the $y = 0.5$ sample, but further systematic investigation with a number of cation-substituted systems is needed to fully understand the factors that control the crystal chemistry of the chemically delithiated layered $Li_{1-x}MO_2$ oxides.

The chemical instability, and the consequent tendency to lose oxygen from the lattice, increases on going from the $y = 0.25$ to the $y = 0.5$ sample. A comparison of the data with the previously reported results for the $Li_{1-x}CoO_{2-\delta}$ and $Li_{1-x}Ni_{0.85}Co_{0.15}O_{2-\delta}$ systems reveals that the chemical instability decreases in the order $Li_{1-x}CoO_{2-\delta} > Li_{1-x}Ni_{0.5}Mn_{0.5}O_{2-\delta} > Li_{1-x}Ni_{0.75}Mn_{0.25}O_{2-\delta} \approx Li_{1-x}Ni_{0.85}Co_{0.15}O_{2-\delta}$, which is consistent with the observed charge voltage profiles. The data suggest that the differences in chemical instability may play a critical role in controlling the practical capacity of the various layered oxides.

Acknowledgment. Financial support by the Welch Foundation Grant F-1254 and the NASA Glenn Research Center is gratefully acknowledged.

CM034757B

(35) Menetrier, M.; Saadoune, I.; Levasseur, S.; Delmas, C. *J. Mater. Chem.* **1999**, *9*, 1135.